DOI: 10.1002/ejic.200700616

(Benzimidazolylmethyl)cyclen: A Potential Sensitive Fluorescent PET Chemosensor for Zinc

Abir El Majzoub,[a] Cyril Cadiou,[a] Isabelle Déchamps-Olivier,[a] Françoise Chuburu,*[a] and Michel Aplincourt[a]

Keywords: Zinc / Macrocyclic ligands / X-ray diffraction / UV/Vis spectroscopy / Fluorescent probes / Fluorimetric titrations

A new fluorescent probe for Zn^{2+}, methylbenzimidazole-pendant cyclen [LH: 1-(benzimidazol-2-ylmethyl)-1,4,7,10-tetraazacyclododecane] was designed and synthesized. The protonation constants of (benzimidazolylmethyl)cyclen and the stability constants of the corresponding zinc complex were determined by potentiometric titrations. The single-crystal X-ray diffraction analysis showed that LH and Zn^{2+} form a 1:1 complex $[ZnLH]^{2+}$. The results of potentiometric, ^1H NMR and UV titrations indicated that above pH 8, $[ZnLH]^{2+}$ mainly deprotonates into $[ZnL]^+$. On addition of successive amounts of Zn^{2+} at pH 10.4 (2×10^{-2} mol L^{-1} CAPS, 25 °C), the fluorescence emission of cyclen(methylbenzimidazole) increases linearly by a factor of 3.

Introduction

The design and synthesis of fluorescent chemosensors is an active field of research and is of particular significance in analytical chemistry since fluorimetric analysis offers a simple method for detecting chemical species in solution.[1] Thus, the development of selective analytical reagents, which allows the quantitative analysis of trace metal ions, is very important for environmental and biological applications. Fluorescent chemosensors developed for the detection of pH and metal cations in aqueous solution generally comprise a fluorophore covalently linked to an ionophore that can bind H^+ or metal cations.[2–5] The principle on which the so-called fluoroionophore works is based on an enhanced or quenched fluorescence of the system when the ionophore units bind H^+ or metal ions. Among the metal ions, the detection of biologically important divalent cations is of great importance to elucidate their physiological roles. In particular, the detection of Zn^{2+}, which is the second most abundant transition metal, following iron, in biological systems, is of interest.[6,7] The most important and best-known role for zinc is as a structural cofactor in metalloproteins. Many zinc proteins possessing one or more zinc motifs have been identified.[8] In these different structures, the zinc environment is usually tetracoordinate {i.e. $[Zn(Cys)_4]$, $[Zn(Cys)_3(His)]$, $[Zn(Cys)_2(His)_2]$}. A catalytic role was also demonstrated for zinc, for instance, in carbonic anhydrase or carboxypeptidase.[9,10] The main difference in the coordination sphere of zinc when its catalytic function is involved is the existence of a vacant coordination site. Recently, the neurological roles of zinc have attracted much attention.[11] A disorder in the metabolism of zinc is closely associated with neurological diseases such as Alzheimer's disease, amyotrophic lateral sclerosis, Parkinson's disease and epilepsy. Thus, there is a great interest in developing zinc sensors, and since, unlike biological metal ions, Zn^{2+} does not give any spectroscopic or magnetic signals (as a result of its d^{10} configuration), fluorescence spectroscopy stands out as a method of choice. Up to now, the reported zinc sensors are chelation-enhanced fluorescent probes.[12–17] Among them, Zn-chelating macrocyclic compounds such as cyclen (1,4,7,10-tetraazacyclododecane) form stable Zn^{II} complexes in aqueous solution at neutral pH. Moreover, by comparison with quinoline-based compounds such as TSQ [6-methoxy-8-(*p*-toluenesulfonamido)-quinoline] and zinquin,[12,13a] for which zinc complexation at neutral pH is not stoichiometric (mixture of ZnL and ZnL_2 complexes can be obtained), cyclen derivatives such as anthracene-pendant cyclen,[14] dansylamide-pendant cyclen,[15] (anthrylmethylamino)ethyl cyclen,[16] 2-[8-hydroxy-5-(dimethylaminosulfonyl)quinolinyl]methyl cyclen[17] complex with almost 100% of Zn^{II} to form ZnL under physiological conditions (at pH 7.4, $10.7 < \log K_{app}$, $[ZnL] < 14.1$, where L represents the ligand and $K_{app[ZnL]} = [ZnL]/[L]_{free}[Zn]_{free}$). The $\log K_{app[ZnL]}$ value depends whether Zn^{2+} is coordinated to the fluorescent unit. Furthermore, from the fluorescent point of view, comparison of the efficiency of the sensors indicates that coordination of the fluorophore to the metal improves the signal.

[a] GRECI, Université de Reims Champagne-Ardenne,
B. P. 1039, 51687 Reims Cedex 2, France
E-mail: francoise.chuburu@univ-reims.fr

Supporting information for this article is available on the WWW under http://www.eurjic.org or from the author.

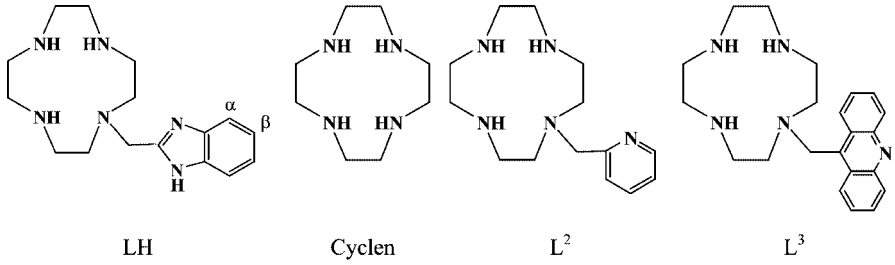

LH Cyclen L^2 L^3

Scheme 1.

Therefore, on the basis of this analysis, we present here a new fluorophore, LH (Scheme 1), in which the ionophore unit is cyclen; according to the affinity for the imidazole of histidine units in metalloenzymes of zinc, we have chosen a benzimidazole moiety as the fluorophore. This paper describes the synthesis and the coordination properties of the resulting (benzimidazolylmethyl)cyclen; protonation and coordination properties towards Zn^{2+} are studied. Spectrophotometric and spectrofluorimetric investigations of the ligand in the presence of Zn^{2+} are also reported in order, first, to test whether the benzimidazole moiety is a good candidate for the detection of zinc and, second, whether the system is responsive in the biological pH window.

Results and Discussion

The ligand LH was prepared following the bisaminal methodology.[18]

Acidity Constants of LH Determined by Potentiometric pH, UV and ^{1}H NMR Titrations

Typical potentiometric pH titration curves of a mixture of (LH) 2×10^{-3} mol L^{-1} and (HNO_3) 10^{-2} mol L^{-1} with I = 1 (KNO_3) at 25 °C were analysed for acid–base equilibrium [Equation (1)]. Four protonation constants were determined for LH by using the PROTAF software (Table 1).[19] The LH macrocyclic cavity protonation assignment was made on the basis of the variation in the cyclen protonation constants upon *N*-functionalisation in relevant ligands L^2 and L^3[20,21] (Table 1). Since the presence of electron-withdrawing pendant groups results in the lowering of the cyclen protonation constants $\log K_{011}$ and $\log K_{012}$, one can conclude that the second and the third protonations of LH ($\log K_{012}$ = 10.21 and $\log K_{013}$ = 9.01) correspond to those of the macrocycle. The fourth protonation constant ($\log K_{014}$ = 4.55) cannot be associated to the cyclen moiety but to the benzimidazole ring. Effectively, this $\log K$ value has to be compared to the $\log K$ value determined for protonation of the pyrrole nitrogen atom in the benzimidazole ring [$\log K_{012}$ (benzimidazole BIH ⇆ benzimidazolium BIH_2^+) ≈ 5.6, see Scheme 2].[22,23] Furthermore, this value is close to that determined for the protonation of the exocyclic pyridine or acridine nitrogen atom of L^2 and L^3, respectively ($\log K_{013}$ = 3.42 and 4.44, respectively, Table 1).[21] In order to get a more precise insight into the acid–base properties of LH before pH 6, the UV absorption changes that take place upon protonation of the macrocyclic nitrogen atoms and/or the benzimidazole moiety were investigated in the 250–340 nm range (Figure 1). In this range and at pH = 6, the electronic spectrum is characteristic of the benzimidazole moiety, and two main absorptions are centred at 273 and 280 nm.[24] This absorption pattern ressembles that of a substituted benzene derivative: two absorption bands are observed in the near UV region that can be assigned to the $\pi^* \leftarrow \pi$ singlet–singlet transitions[25]($^1L_a \leftarrow S_0$ and $^1L_b \leftarrow S_0$, where ^1L_a and ^1L_b correspond to the two excited states[25c]). The extinction coefficients (ε_{max} = 6700 mol^{-1} L cm^{-1} at 273 and 280 nm) are in agreement

Table 1. Ligand protonation constants $\log K_{0/h}$.[a]

		LH[b]	Cyclen[c]	L^{2}[d]	L^{3}[e]
L[f] + H^+ ⇌ LH	$\log K_{011}$	11.05(4)	10.97	10.6	10.32
LH + H^+ ⇌ LH_2	$\log K_{012}$	10.21(8)	9.87	9.77	7.78
LH_2 + H^+ ⇌ LH_3	$\log K_{013}$	9.01(5)	<2	3.42	4.44
LH_3 + H^+ ⇌ LH_4	$\log K_{014}$	4.55(9)	<2	<2	<2
LH_4 + H^+ ⇌ LH_5	$\log K_{015}$	<2	–	<2	<2
LH_5 + H^+ ⇌ LH_6	$\log K_{016}$	<2	–	–	–

[a] The numbers in parentheses refer to the estimated standard deviations for the last significant digit (95% confidence). [b] Potentiometric titrations at 25.0(1) °C, I = 1 (KNO_3) (this work). [c] Ref.[20] [d] Ref.[21a] [e] Ref.[21b] [f] For LH, the L species corresponds to the anionic form of the ligand.

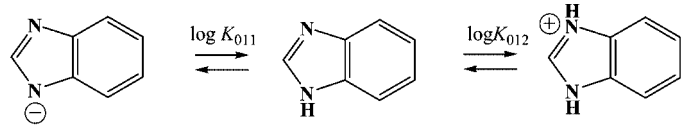

BI^- BIH BIH_2^+

$\log K_{011}$(25°C) = 12.75 [22]; 12.78 [27] $\log K_{012}$ (25°C) = 5.58 [23]; 5.68 [23]

Scheme 2.

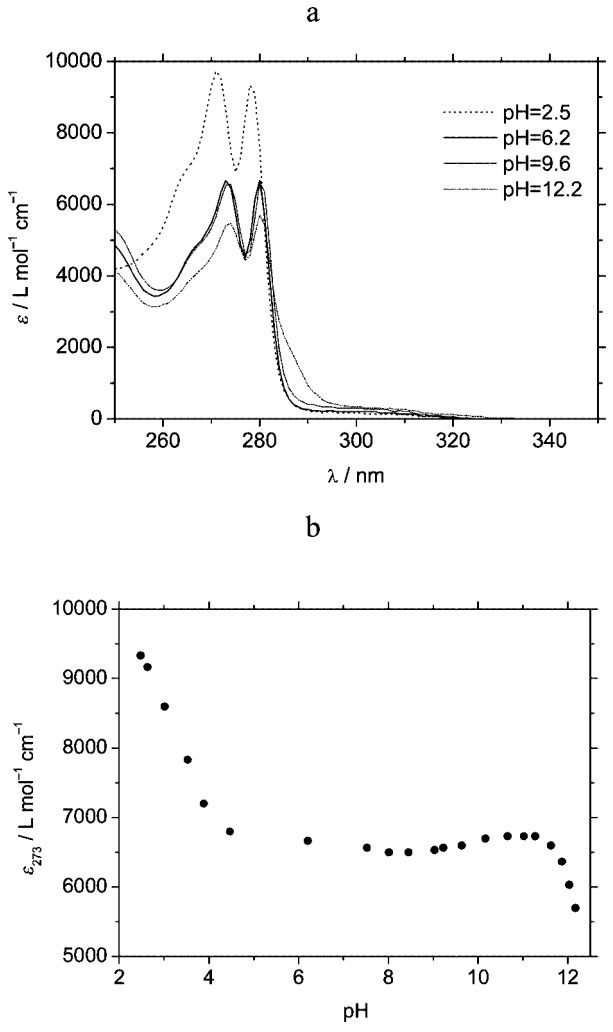

Figure 1. (a) Spectrophotometric titration of LH with KOH (0.1 mol L^{-1}): [LH] = 3×10^{-5} mol L^{-1} in HCl (10^{-2} mol L^{-1}), T = 25 °C, path length = 1 cm; (b) ε_{273} (mol^{-1} L cm^{-1}) as a function of pH.

with those obtained in bis(benzimidazole) macrocycles.[25,26] Acidification of the medium down to pH = 6 induces perturbations in the spectra: the previous bands undergo a slight blue shift (λ = 2 nm) similar to that observed for the free benzimidazole under acidic conditions.[24] This slight shift is accompanied by a strong hyperchromic effect, which results in an approximately 50% increase in the parent extinction coefficient (Figure 1b). This effect can be compared to the hyperchromic effect observed under similar conditions on the $\pi^* \leftarrow \pi$ transition of cyclen- and cyclam–pyridine.[21a] This result is characteristic of the formation of a benzimidazolium cation. This analysis can be consolidated by the change in the ^{1}H chemical shifts of H_α and H_β of the benzimidazole moiety (for the numbering see Scheme 1) in the pH range 6.2–2.5 in D_2O (Supporting Information Figure S1). The decrease in pH is accompanied with a downfield shift of the signals of the aromatic protons as expected for protonation of the aromatic ring.[21a] These convergent observations imply that the log K value of 4.55 can be attributed to protonation of the benzimidazole group.

Finally, the first protonation constant (log K_{011} = 11.05) determined for (benzimidazolylmethyl)cyclen LH cannot be attributed to the cyclen moiety but to the benzimidazole ring. This is supported by UV and ^{1}H NMR spectroscopic experiments above pH 9. The increase in pH is accompanied by an upfield shift in the NMR spectrum of the signals for the aromatic protons (Supporting Information, Figure S1). Accordingly, in the range 250–290 nm in the absorption spectrum, a hypochromic effect is observed with a slight red shift of the bands (Figure 1), and a low-energy shoulder appears at 287 nm. These data are in agreement with the formation of a benzimidazolate species (Scheme 2).[24,27] From the sigmoidal curve observed in the plot of ε_{273} versus pH (Figure 1b), one can estimate the corresponding log K value to be 11, which agrees well with the

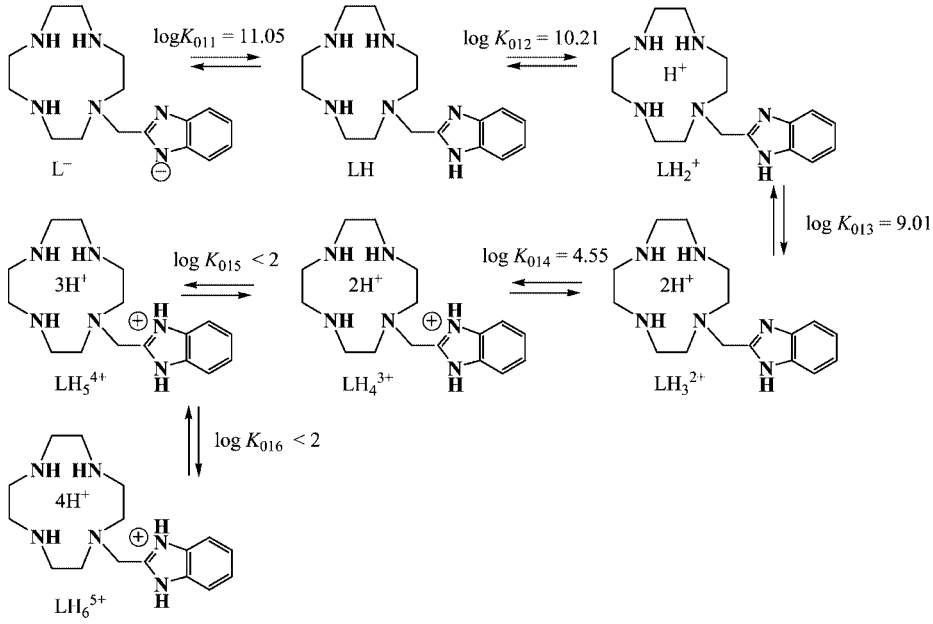

Scheme 3.

$\log K_{011}$ value obtained from the potentiometric pH titration. On the basis of these results, the acid–base behaviour of LH is summarised in Scheme 3.

Zinc(II) Complex of LH

Synthesis and Solid-State Structure of [ZnLH](ClO$_4$)$_2$

[ZnLH]X_2, where X = NO_3 and ClO_4, were synthesised by reacting one equivalent of the ligand and one equivalent of the $ZnX_2{\cdot}nH_2O$ salt in a methanolic solution. Colorless single crystals were obtained only for [ZnLH](ClO$_4$)$_2$ by diffusion of diethyl ether in an acetonitrile solution of the complex. Selected geometrical parameters for [ZnLH](ClO$_4$)$_2$ are given in Table 2. The X-ray structure of $[ZnLH]^{2+}$ shows that the metal ion lies inside a square-based pyramid (Figure 2) and that the coordination sphere of the zinc centre consists of the four macrocyclic nitrogen atoms (N1–N4) and the imine nitrogen atom of the benzimidazole (N_{im}). The Zn^{II} cation lies 0.781 Å above the macrocyclic nitrogen square in this distorted square-based pyramid geometry. The Zn–N(secondary) bonds (2.104–2.116 Å) are shorter than the Zn–N(tertiary) bond (2.236 Å): tertiary nitrogen atoms are not as good donors as secondary nitrogen atoms.[28–30] The N_{im} atom is coordinated to the zinc cation. This type of coordination in which the imidazole is linked to the metal cation through the imine nitrogen atom and the hydrogen atom of the secondary amine nitrogen atom remains is well known for histidine and nucleoside bases such as adenine and guanine.[10] The Zn–N_{im} bond of 1.982 Å is shorter than the Zn–N(cyclen) bonds, which indicates a strong interaction between the N_{im} and Zn^{II} atoms. This feature has already been reported for a Zn–guanidinyl cyclen complex in which the Zn–N(guanidyl) bond[31] (1.95 Å) is shorter than the average Zn–N(cyclen) bonds (2.16 Å). For $[ZnLH]^{2+}$ in the solid state, an efficient five-membered chelate ring is formed, as the N_{im}–Zn–N4 angle of 80.6° is noticeably smaller than the other three N_{im}–Zn–N angles (104.6–138.2°). This indicates that electron donation from the imine nitrogen lone pair of the benzimidazole moiety to the Zn^{II} ion is strong. Furthermore, comparison of the C–N bond lengths in the imidazole ring of $[ZnLH]^{2+}$ (C2–N_{im}: 1.324 Å and C2–N_{am}: 1.347 Å) and in free benzimidazole[32] (C2–N_{im}: 1.297 Å and C2–N_{am}: 1.344 Å) shows that the C2–N_{im} distance is elongated by coordination. This indicates an electronic delocalisation through the imidazole ring,[33] which results in the reinforcement of the electronic density at the N_{im} nitrogen atom (Scheme 4). The driving force of this phenomenon is the Zn^{II} Lewis acidity. Finally, to ensure the cohesion of the solid-state structure, hydrogen bonds between ClO_4^- oxygen atoms and N1, N3 and N_{am} hydrogen atoms are present.[34]

Table 2. Selected bond lengths [Å] and angles [°] for $[ZnLH]^{2+}$.

Zn–N1	2.1049(15)	N1–Zn–N2	83.25(6)
Zn–N2	2.1147(15)	N1–Zn–N3	133.47(6)
Zn–N3	2.1163(16)	N1–Zn–N4	81.22(6)
Zn–N4	2.2369(15)	N1–Zn–N_{im}	114.79(6)
Zn–N_{im}	1.9829(15)	N2–Zn–N3	83.42(6)
N_{im}–C2	1.324(2)	N2–Zn–N4	141.03(6)
N_{am}–C2	1.347(7)	N2–Zn–N_{im}	138.19(6)
		N3–Zn–N4	81.85(6)
		N3–Zn–N_{im}	104.64(6)
		N4–Zn–N_{im}	80.60(6)

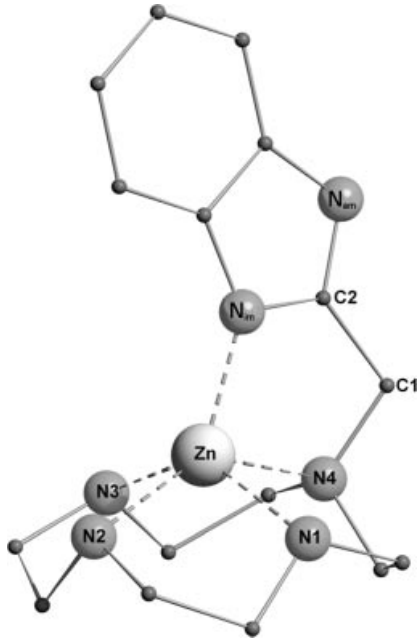

Figure 2. Schakal diagram of $[ZnLH]^{2+}$ (hydrogen atoms are omitted for clarity, with the exception of the H atom of N_{am}).

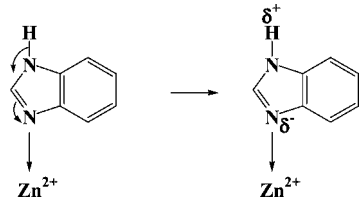

Scheme 4.

Thermodynamic Stability of the Zn^{II}-LH Complex – Potentiometric pH, UV and ^{1}H NMR Titrations

At first, direct pH titrations of LH in the presence of one equivalent of Zn^{2+} and a strong acid in excess were carried out following a published procedure for similar compounds.[35] By using this method with LH, we encountered some problems because Zn^{2+}complexation is very slow at low pH. This can be attributed to the protonation of the ligand nitrogen atoms (the macrocyclic nitrogen atoms and the pyrrole nitrogen atom in the benzimidazole ring). In order to counteract this drawback in acidic medium, the "batch method", which involves the preparation of LH/

$Zn^{2+}/HNO_3/KOH$ mixtures at each pH value, was then used.[36] This method was implemented up to pH 7, after which carbonation cannot be avoided. Direct KOH titrations of synthesised $[ZnLH]^{2+}$ were also carried out in the pH range 5–12. For comparison, similar titrations were performed with pendantless cyclen. From the analysis of the titration data, the speciation diagram of the Zn^{2+}/LH system was obtained (Figure 3), and the values for the overall complexation constants of the 1:1 Zn^{II} complex ($\log\beta_{mlh}$) calculated (Table 3). Firstly, the speciation diagram indicates that there is no formation of the Zn^{II} complex with LH_4^{3+} in acidic medium. This is confirmed by spectroscopy: the UV (Figure 4) and/or ^1H NMR (Figure 5 and Supporting Information Figure S2) experiments show that, under acidic conditions, the presence of the metal does not affect the signal, since the ligand is the only species detected. Secondly, the diagram indicates that at pH 3, the $[ZnLH]^{2+}$ complex starts to form: this is confirmed by ^1H NMR spectroscopy, since in the ^1H NMR spectrum, a second set of signals at δ = 7.64, 7.38 and 4.28 ppm increasingly appears, while the signals for LH collapse (from pH 3.7). Comparison of the LH and cyclen affinities for Zn^{2+} before pH 4 (Supporting Information Figure S3) indicates, moreover, that the presence of the benzimidazole moiety on the cyclen framework promotes Zn^{2+} complexation in acidic medium. The speciation diagram highlights that the 1:1 Zn^{II} complex is quantitatively obtained between pH 5–7. In this pH range, the UV and ^1H NMR spectra remain unchanged. From the $\log\beta_{111}$ value and the first protonation constant, $\log K_{011}$, of the ligand, the stepwise formation constant of the species $[ZnLH]^{2+}$ was calculated to be 16.13 (Table 3). This value is higher than that of the cyclen complex $\{\log K_{[Zn(cyclen)]} = 14.20\}$. The affinity of LH for Zn^{2+} is greater than that of cyclen over the whole pH range (Supporting Information Figure S3). Usually, the *N*-functionalisation of the tetraazamacrocycle induces a decrease in the stability of the complexes, which results mainly because of the poor σ-donor ability of tertiary amines relative to that of secondary amines.[16,30,38,39] Here, the enhanced stability of $[ZnLH]^{2+}$ must be due to the presence of an additional stabilising interaction, probably between the benzimidazole ring and the metal through a supplementary five-membered ring chelate. This also suggests that the solid-state structure remains in solution. Although lower, the stability of $[ZnLH]^{2+}$ compares well with that determined for the [{(anthrylmethylamino)ethyl}cyclen]Zn^{II} complex ($\log K$ = 17.6).[16] This stability is even lower than that of the [{8-hydroxy-5-(dimethylaminosulfonyl)quinolin-2-

Table 3. Stability constants for the Zn^{II}/LH and Zn^{II}/cyclen systems.

Equilibrium	LH $\log\beta_{mlh}$	Cyclen[a] $\log\beta_{mlh}$
Zn + L + H^+ ⇌ ZnLH	27.18(8)	
Zn + L ⇌ ZnL	18.53(6)	14.20(8) (15.3[35])
Zn + L ⇌ ZnL(OH) + H^+	7.5(3)	6.3(1) (7.44[37])
	$\log K$	
Zn + LH ⇌ ZnLH	16.13	
ZnLH ⇌ ZnL + H^+	–8.65	

[a] Potentiometric titrations at 25.0(1) °C, I = 1 (KNO_3) (this work).

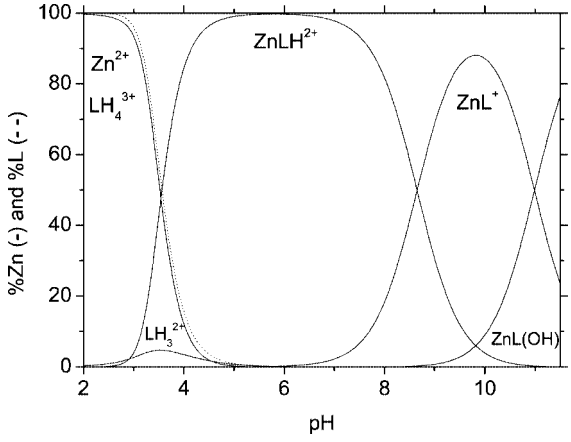

Figure 3. Speciation diagram of the Zn^{II}/LH system as a function of pH ($[Zn^{II}]$ = [LH] = 2×10^{-3} mol L^{-1}). The dashed line corresponds to Zn^{2+}.

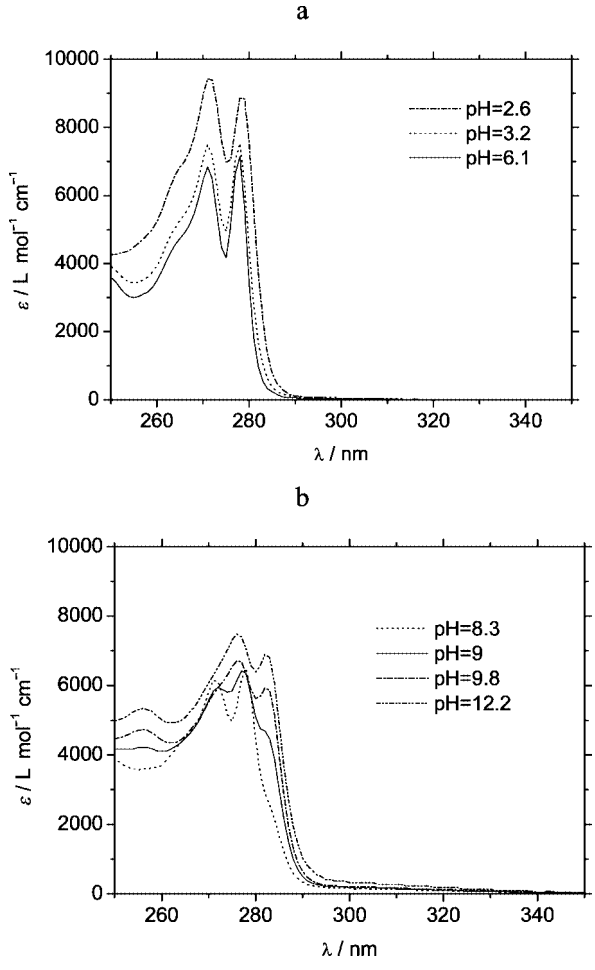

Figure 4. Spectrophotometric titration of $[ZnLH]^{2+}$ with KOH (0.1 mol L^{-1}): (a) $[ZnLH]^{2+}$ = 3×10^{-5} mol L^{-1} in HCl (10^{-2} mol L^{-1}), pH range 2.6–6.1; (b) $[ZnLH]^{2+}$ = 3×10^{-5} mol L^{-1}, pH range 7–12.2. T = 25 °C; path length = 1 cm.

ylmethyl}cyclen]Zn^{II} complex ($\log K$ = 22.4).[17] It can be assumed for the latter that the enhanced stability is due to the fact that the metal ion is six-coordinate rather than five-coordinate. Another way to compare the thermodynamic behaviour of different systems is to calculate the apparent complexation constant $\log K_{app}$ at a given pH. The $\log K_{app}$ value is calculated from the potentiometric pH titration results, according to $\log K_{app} = \log([ZnLH]/[Zn]_{free} \times [L]_{free})$ with $[L]_{free} = \sum_n [H_nL]_{free}$ (n = 0–4 for LH) and for an equimolar mixture of 5×10^{-6} mol L^{-1} LH and Zn^{2+}. At pH 7.4, in the medium of the biological pH window, the $\log K_{app[ZnLH]}$ value is calculated to be 11.71. This value is between those calculated under the same conditions for [{(anthrylmethylamino)ethyl}cyclen]Zn^{II} complex ($\log K_{app[ZnL]}$ = 10.7)[16] and for [{8-hydroxy-5-(dimethylaminosulfonyl)quinolin-2-ylmethyl}cyclen]Zn^{II} complex ($\log K_{app[ZnL]}$ = 14.1).[17] Finally, above pH 8, the deprotonation of $[ZnLH]^{2+}$ was confirmed by ^1H NMR and UV spectroscopy. Thus, around pH 8.5, the ^1H signals for H_α, H_β and $N_{cyclen}CH_2$ are shifted upfield [Figure 5: $\Delta(\delta)$ = 0.15 ppm for H_α, 0.25 ppm for H_β and 0.3 ppm for $N_{cyclen}CH_2$]. This shielding indicates a decrease in the overall charge of the complex. Accordingly, on increasing the pH up to 12, the UV bands of the benzimidazole unit are perturbed and undergo a slight red shift of about 5 nm (Figure 4b). As indicated for the ligand, this is characteristic of deprotonation at the imidazole ring.[24] Moreover, a new band appears at 282 nm from pH 8, and up to pH 12, the extinction coefficient of this band increases by about a factor of six. From the $\log \beta_{mlh}$ values, one can calculate the deprotonation constant of $[ZnLH]^{2+}$ ($\log K$ = –8.65), which, as suggested by the UV titration, corresponds to the ionisation of the pyrrole hydrogen of the benzimidazole moiety. This value is remarkably lower than that for the analogous equilibrium in LH, which means that in the presence of Zn^{II}, the benzimidazole pyrrole hydrogen is $10^{2.4}$ times more acidic. This is a consequence of the Lewis acidity of the Zn^{II} ion, which operates predominantly through an inductive effect and strongly alters the benzimidazole acidity.[40]

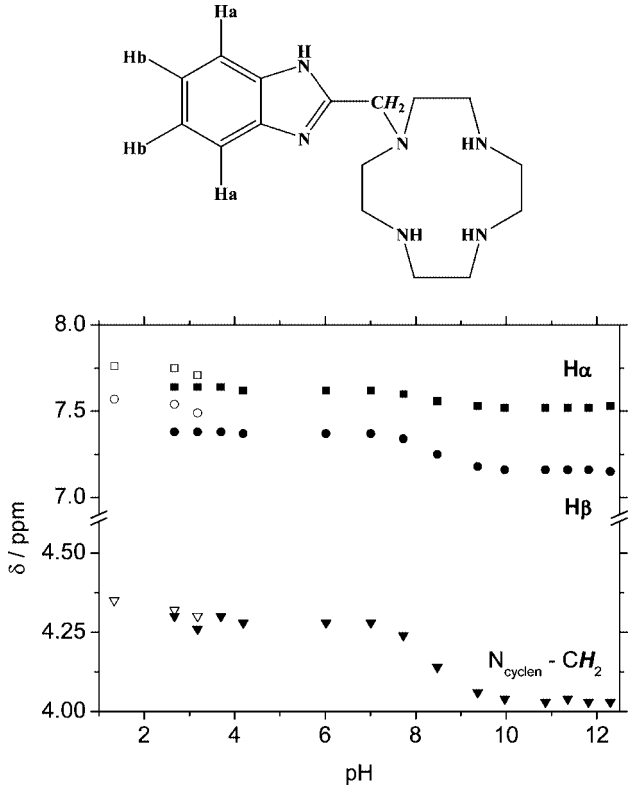

Figure 5. ^1H NMR chemical shifts plotted as a function of pH for a mixture of LH (10^{-2} mol L^{-1}) and Zn^{2+} (10^{-2} mol L^{-1}) in the pH range 3.0–12.0 (T = 25 °C, D_2O). The filled symbols correspond to the complex chemical shifts.

Spectrofluorimetric Study of LH

The change in the fluorescent response of LH (5×10^{-7} mol L^{-1}) in the pH range 4–12 (I = 0.1 $NaNO_3$) at 25 °C (excitation at 270 nm) is presented in Figure 6. Inspection of the LH deprotonation sequence indicates that the fully protonated species gives rise to the smallest emission intensity and that removal of the protons leads to an increase in the fluorescence emission intensity. Thus, as the pH is raised, emission at 301 nm increases following a sigmoidal curve with an inflexion point at pH 9. The fluorescence curve follows the formation of all the species in solution at pH > 8, i.e. LH^{2+}, LH and L^-. It is concluded that the break at pH 9 in Figure 6 denotes the pK_{a4} for $LH_3^{2+} \leftrightarrows LH_2^+$. The further increase in the fluorescence emission (above pH 10.5) is due to deprotonation at the benzimidazole moiety. Consequently, the quantum yield Φ of (benzimidazolylmethyl)cyclen increases with the pH from 0.21 at pH 10.4 to 0.30 at pH 12. The enhanced effect of the fluorescence emission can be explained in terms of an intramolecular electron-transfer process from the macrocycle to the excited benzimidazole (PET process).[41] Such a mechanism involves the deactivation of the excited state of the fluorophore by addition of one electron to one of its excited-state frontier orbitals. This leaves the fluorophore in a reduced, nonemissive state. Among factors responsible for intramolecular electron transfer, the overlap S between the electron donor (macrocycle) and acceptor (benzimidazole) orbitals is, of course, crucial, and it is obvious that S is optimum when both parts of the fluoroionophore are in close proximity and in a suitable orientation. In functionalised macrocycles, it has already been shown that protonated forms of the macrocycle are stabilised by intramolecular hydrogen bonds between the cavity and the pendant arm when the latter has coordinating atoms.[21a,42] Furthermore, deprotonation at the cavity induces conformational modifications in the ligand that lead to an outward orientation of the pendant arm relative to the macrocyclic cavity. If we assume that similar conformational changes occur during deprotonation of LH, in particular between the LH_3^{2+}, LH_2^+ and LH species, then an increase in the distance between the cavity and the benzimidazole moiety results. One can then

explain the fluorescence enhancement observed during the deprotonation sequence by the reduced overlap of the orbitals of both parts of the fluoroionophore, which favours the emissive deactivation of benzimidazole over the PET process.

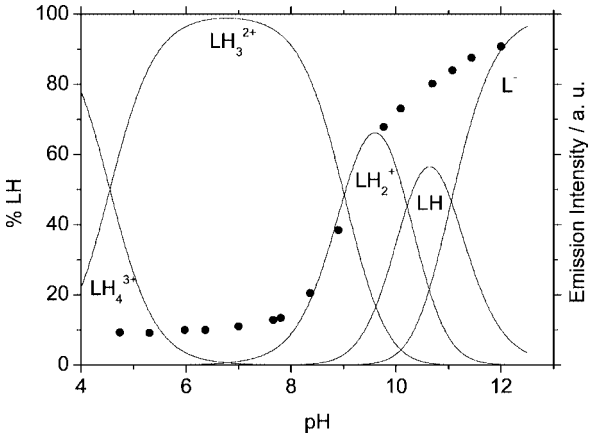

Figure 6. Speciation diagram of the LH system as a function of pH in the pH range 4.0–12.0, and the fluorescent response of LH (5×10^{-7} mol L^{-1}).

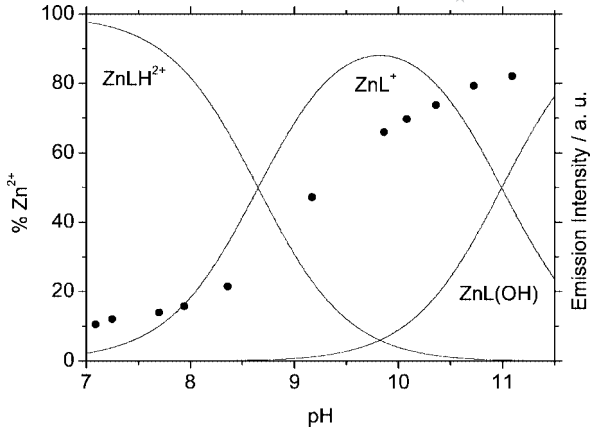

Figure 7. Speciation diagram of the LH/Zn^{2+} system as a function of pH in the pH range 7.0–12.0, and fluorescent response of LH/Zn^{2+}.

Moreover, once formed $[ZnL]^+$ is so stable that even at such concentrations, the 1:1 complex does not dissociate and the Zn^{2+}-dependent fluorescence is unaffected by excess amounts of Zn^{2+}.

Fluorescence of $[ZnLH]^{2+}$ and Titration of LH with Zn^{2+}

The change in the fluorescence emission of the zinc complex (5×10^{-7} mol L^{-1}) as a function of pH is presented in Figure 7. The fluorescence curve follows the formation of all the species in solution at pH >8, i.e. ZnL^+, ZnL(OH). The sensitivity of the fluorescence in the complex implicates deprotonation at the benzimidazole moiety. This behaviour should be compared with that of [(dansylamidoethyl)-cyclen]Zn.[15] Moreover, the emission of LH increased by about a factor of three with increasing $[Zn^{2+}]$ (quantum yield Φ 0.21 → 0.63). This chelation-enhanced fluorescence can be explained as follows: the metal coordination induces an energetic modification of the molecular orbitals between the free macrocycle and the corresponding Zn^{II} complex that leads to the stabilisation of the HOMO. Consequently, the Zn-cyclen subunit is a less efficient donor towards the benzimidazole fluorophore than the cyclen unit in LH towards the same benzimidazole moiety. This makes PET-type fluorescence quenching less probable, and the native fluorescence of the fluorophore is thus restored.[43]

In order to test the response of LH in the presence of Zn^{2+}, it is then necessary to follow the fluorescence emissionat pH 10.4 where, first, a significant alteration in the signal intensity in response to the binding unit is expected, and, second, the complexation kinetics is fast. The change in fluorescence upon addition of Zn^{2+} to (benzimidazolylmethyl)cyclen is presented in Figure 8. Upon excitation at 270 nm, an increase in emission is observed. The response of the system at 301 nm is linear between 5×10^{-8} and 5×10^{-7} mol L^{-1}, until a 1:1 [LH]/$[Zn^{2+}]$ ratio is reached. This implies that the increase in fluorescence is stoichiometric and is due to total formation of the $[ZnL]^+$ complex.

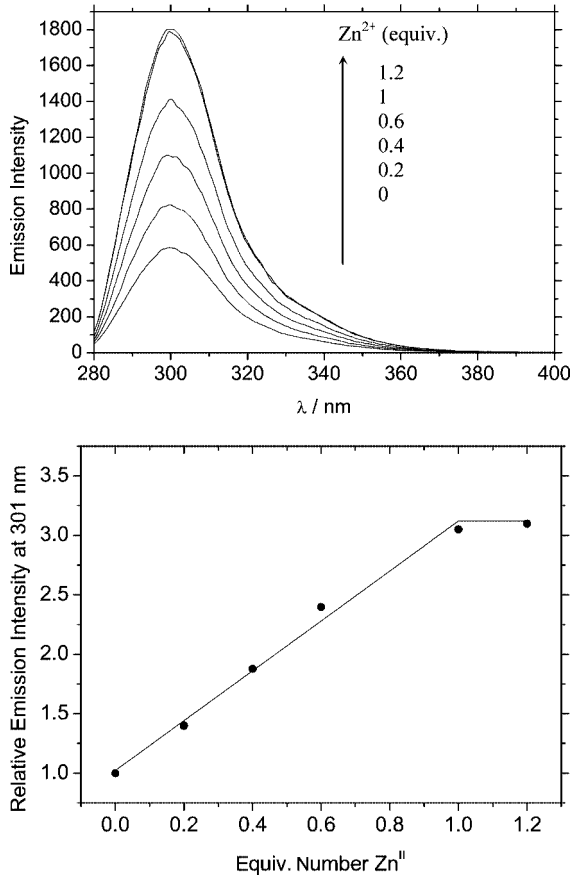

Figure 8. Change in the fluorescent response of LH (5×10^{-7} mol L^{-1}) upon addition of Zn^{2+} at pH 10.4 [CAPS (2×10^{-2} mol L^{-1}), I = 1 ($NaClO_4$), T = 25 °C, excitation at 270 nm].

To determine whether LH works as a selective chemosensor for Zn^{2+}, the LH fluorescent spectra were recorded in the presence of various metal ions at pH 10.4 (some first-row transition metals, Cd^{II} and biologically relevant alkali and alkaline earth ions, Figure 9). The fluorescent intensities slightly increase by addition of ions that are found in high concentrations in cells, such as K^+, Mg^{2+} and Ca^{2+}. The selectivity of Zn^{2+} over alkali or alkaline earth cations comes from the inherent binding properties of macrocyclic polyamines. Addition of transition metals such as Mn^{2+} and Fe^{3+} does not significantly increase the fluorescent response of (benzimidazolylmethyl)cyclen. This test also indicates that the cadmium complex is less fluorescent than the ligand (which allows Zn^{2+} and Cd^{2+} to be distinguished), while the copper complex does not fluoresce at all. For these two cations, the decrease in fluorescence is due to a quenching mechanism.[44]

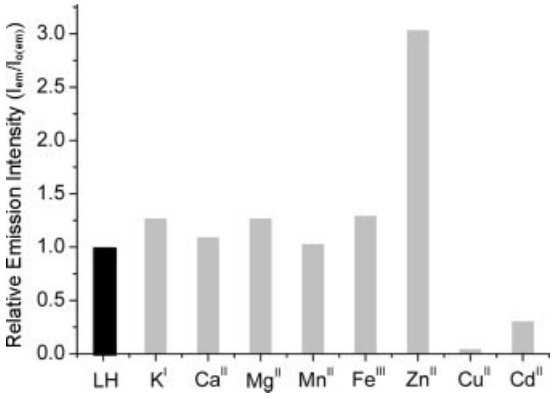

Figure 9. Relative fluorescence of LH at 301 nm responding to 1 equiv. of the metal ions at pH 10.4 [CAPS (2×10^{-2} mol L^{-1}), I = 1 (NaCl), T = 25 °C, excitation at 270 nm]. $I_{0(em)}$ is the emission intensity of LH (5×10^{-7} mol L^{-1}) at 301 nm in the absence of metal ions.

In comparison with the results reported for cyclen fluorophores,[15–17] the fluorimetric titration of Zn^{2+} with LH shows that LH does not respond to Zn^{2+} at neutral pH, which is a disadvantage. This point has to be improved in order to envisage a use under biological conditions. For that, the key mechanistic feature is the decoupling of macrocyclic electron-donor nitrogen atoms from resonance with the fluorophore. In light of the behaviour of the anthracene-pendant cyclen probe, which responds to Zn^{2+} for pH values >12,[14] and the {(anthrylmethylamino)ethyl}-cyclen probe, which responds to Zn^{2+} at neutral pH,[16] the introduction of an aminoethyl spacer between the macrocycle and the methylbenzimidazole moiety is to be studied. The introduction of a supplementary amine function on the spacer is expected to sufficiently change the electronic nature of the ligand and complex structures at neutral pH to be able to detect Zn^{2+} under better conditions.

Conclusions

We have designed a new ligand LH for complexation with Zn^{2+} and that can be detected by fluorescence spectroscopy. The zinc(II) complex is stable and quantitatively formed at pH 5, which is comparable to zinc(II) complexes obtained from (dansylamidoethyl)cyclen[15] or {(anthrylmethylamino)ethyl}cyclen.[16] The complexation induces a PET-retarded fluorescence, which is responsible for the fluorescence enhancement in the presence of Zn^{2+}. Thus, in CAPS buffer and upon addition of increasing amounts of Zn^{2+}, the fluorescent emission of LH linearly increases. The detection limit of LH (5×10^{-7} mol L^{-1}) is [Zn^{2+}] = 5×10^{-8} mol L^{-1} at pH 10.4. The LH fluorescent response to Zn^{2+} has to be improved in order to allow Zn^{2+} detection at neutral pH. On the basis of the modification of the ligand already proposed by Aoki and al.,[16] it is envisaged that the introduction of an aminoethyl spacer between the macrocycle and the methylbenzimidazole moiety will help towards this end.

Experimental Section

General Information: All solvents were HPLC grade. The metals salts were purchased from Aldrich. The other reagents (highest commercial quality) were used without further purification.

Ligand Synthesis: The ligand LH was synthesised according to a published procedure[18] by alkylation of the cyclen glyoxal ligand (5.1 mmol, 1.00 g) with 2-(chloromethyl)benzimidazole (5.3 mmol, 0.89 g) in thf. The solution was stirred for 6 h, after which a pale yellow precipitate forms, which corresponds to the alkylated bisaminal monosalt. This was separated from the mother solution by filtration. This salt was then deprotected with hydrazine monohydrate for 3 h at 100 °C. After cooling, a brown oil precipitates, which was collected by filtration and washed several times with ethanol. The ligand LH was finally obtained after purification in methanol in 53% yield (0.87 g). ^{13}C NMR (62.9 MHz, D_2O): δ = 44.5, 45.4, 51.4, 52.8 and 73.7 (CH_2N), 115.2, 123.2, 118.1 and 153.9 (C_{Ar}) ppm. $C_{16}H_{26}N_6\cdot0.25CH_3OH\cdot0.5H_2O$ (319.44): calcd. C 61.10, H 8.84, N 26.31; found C 61.09, H 9.14, N 26.67%.

Preparation of the Zinc Complexes

[Zn(cyclen)$(NO_3)_2$]: A methanolic solution of $Zn(NO_3)_2\cdot4H_2O$ (0.61 mmol, 0.16 g, 5 mL) was added dropwise to a solution of the ligand (cyclen: 0.60 mmol, 0.11 g) in methanol (10 mL). The colourless solution was heated at reflux for 4 h and concentrated by evaporation. A white powder was precipitated by addition of diethyl ether solution (0.16 g, 74%). $C_8H_{20}N_4Zn(NO_3)_2$ (361.67): calcd. C 26.57, H 5.57, N 23.24; found C 26.71, H 5.66, N, 23.39%. ESI-MS: m/z calcd. for $[Zn(C_8H_{20}N_4)(NO_3)]^+$ 298.1; found 298.0.

[ZnLH]$(NO_3)_2$: A methanolic solution of $Zn(NO_3)_2\cdot4H_2O$ (0.68 mmol, 0.18 g, 5 mL) was added dropwise to a solution of the ligand (LH: 0.66 mmol, 0.21 g) in methanol (10 mL). The colourless solution was heated at reflux for 4 h and concentrated by evaporation. A white powder was precipitated by addition of diethyl ether solution (0.19 mg, 58%). ^{13}C NMR (62.9 MHz, CD_3OD): δ = 45.1, 42.3, 47.4, 52.2 and 53.9 (CH_2N), 113.5, 118.5, 125.2, 125.8, 135.6, 139.3 and 153.3 (C_{Ar}). $C_{16}H_{26}N_6ZnN_2O_6\cdot0.25CH_3OH$ (499.83): calcd. C 39.05, H 5.44, N 22.42; found C 38.92, H 5.26, N 22.49%.

[ZnLH]$(ClO_4)_2$: A methanolic solution of $Zn(ClO_4)_2\cdot6H_2O$ (0.41 mmol, 0.15 g, 5 mL) was added dropwise to a solution of the ligand (LH: 0.35 mmol, 0.11 g) in methanol (5 mL). The colourless solution was heated at reflux for 4 h and concentrated by evapora-

tion. A white powder was precipitated by addition of diethyl ether (0.10 g, 50%). $C_{16}H_{26}N_6ZnCl_2O_8{\cdot}0.5H_2O$ (575.72): calcd. C 33.38, H 4.73, N 14.60; found C 33.62, H 4.76, N 14.42%. ESI-MS: *m*/*z* calcd. for $[Zn(C_{16}H_{26}N_6)(ClO_4)]^+$ 465.1; found 465.1. This solid was further dissolved in acetonitrile, and after slow diffusion of diethyl ether, white monocrystals of $[ZnLH](ClO_4)_2{\cdot}CH_3CN$ suitable for X-ray analysis were produced.

CAUTION: Perchlorate-containing complexes are potentially explosive and appropriate precautions should be in place for their preparation, handling and storage.

Potentiometric Measurements: Potentiometric titrations were carried out with an automatic titrator composed of a microprocessor burette (Metrohm dosimat 665) and a pH meter (Metrohm 713) connected to a computer. The titration procedure was fully automated.[19] All measurements were performed within a thermoregulated cell at 25.0 ± 0.1 °C under an argon stream to avoid the dissolution of carbon dioxide. The ionic strength was adjusted to 1 with potassium nitrate. The combined Type "U" glass electrode (Metrohm) used had a very low alkaline error. The complex formation constants were determined according to the "batch method". Equimolar mixtures of Zn^{2+} and ligand [2×10^{-3} mol L^{-1} in 10^{-2} mol L^{-1} HNO_3 , I = 1 (KNO_3)] were prepared in 30 stoppered flasks at different pH values by microaddition of KOH [10^{-1} mol L^{-1}, I = 1 (KNO_3)]. These solutions were stored under argon and placed in a thermoregulated enclosure at 40 °C for two, four or six weeks. Before pH measurements, these solutions were allowed to reach equilibrium temperature (25 °C) for 48 h. The deprotonation of the [(benzimidazolylmethyl)cyclen]zinc complex was determined by a pH titration of a complex solution [2×10^{-3} mol L^{-1}, I = 1 (KNO_3)] prepared from the solid $[ZnLH](NO_3)_2$ monohydrate complex previously described.

The protometric data were processed by using the PROTAF program[19] to obtain the best-fit chemical model and refined overall constants, β_{mlh}.

$$mM + lL + hH^+ \rightleftharpoons M_mL_lH_h$$

$$\beta_{mlh} = \frac{[M_mL_lH_h]}{[M]^m[L]^l[H^+]^h}$$

A negative h value refers to the hydroxide ion.

The stepwise protonation constants (K_{0lh}) related to equilibrium (1) are defined by Equation (2) and are deduced from the refined β_{0lh} values by Equation (3).

$$LH_{h-1}^{(h-1)+} + H^+ \overset{K_{0lh}}{\rightleftharpoons} LH_h^{h+} \quad (1)$$

$$K_{0lh} \frac{[LH_h^{h+}]}{[LH_{h-1}^{(h-1)+}][H^+]} \quad (2)$$

$$\beta_{0lh} = \prod_{i=1}^{h} K_{0li} \quad (3)$$

Spectroscopic Measurements: ^{1}H and ^{13}C NMR spectra were recorded with a Bruker DRX 500 spectrometer. ^{1}H–^{1}H and ^{1}H–^{13}C 2D correlation experiments were performed to assign the signals. In ^{1}H NMR titrations, the pD was adjusted by additions of small amounts of a 4-% diluted NaOD solution or a 3.5-% diluted DCl solution to D_2O solutions containing the ligand LH (10^{-2} mol L^{-1}). The pH was calculated from the measured pD values by using Equation (4):[26]

$$pH = pD - 0.40 \quad (4)$$

For both ligands, NMR measurements were performed after an equilibration time of one day. Mass spectra in methanol were recorded on a Micromass Q-TOF electrospray positive ionisation instrument. For both ligand and complex $[ZnLH](ClO_4)_2{\cdot}H_2O$ (3×10^{-5} mol L^{-1}), the UV spectrophotometric titrations were recorded at 25 °C in the range 200–400 nm with a thermoregulated Shimadzu UV 2401 PC spectrophotometer. For the UV pH titrations, the pH was adjusted by addition of small amounts of KOH (10^{-1} to 10^{-3} mol L^{-1}) and HCl solutions (10^{-1} to 10^{-2} mol L^{-1}).

Crystal Structure Determination: The crystal diffraction data were collected at 120 K with a Kappa CCD diffractometer (Centre de Diffractométrie X, Univ. Rennes, France) by using monochromated Mo-K_α radiation (λ = 0.71073 Å). Data collection was performed with the COLLECT program.[45] Frame integration and data reduction procedures were realised with the DENZO and SCALEPACK programs of the KappaCCD software package, respectively,[46] for the [ZnLH] compound and with EVAL[47] and SADABS[48] programs, respectively. The structure was solved by using the direct methods program SIR97,[49] which revealed all non-hydrogen atoms. SHELXL97[50] was used to refine the structure. Finally, hydrogen atoms were placed geometrically and held in riding mode in the least-squares refinement procedure. Final difference maps revealed no significant maxima (Table 4). CCDC-648571 contains the supplementary crystallographic data for this paper. These data can be obtained free of charge from The Cambridge Crystallographic Data Centre via www.ccdc.cam.ac.uk/data_request/cif.

Table 4. Crystal data and details of the structure determination for $[ZnLH](ClO_4)_2{\cdot}CH_3CN$.

	$[ZnLH](ClO_4)_2{\cdot}CH_3CN$
Empirical formula	$C_{18}H_{29}Cl_2N_7O_8Zn$
Formula weight	607.75
Temperature [K]	100(2)
Crystal system	monoclinic
Space group	*P*21/*c*
colour	colourless
a [Å]	14.7457(4)
b [Å]	9.2669(3)
c [Å]	18.7281(6)
α [°]	90
β [°]	106.5910(10)
γ [°]	90
Volume [Å^3]	2452.59(13)
Z	4
$D_{calcd.}$ [g cm^{-3}]	1.646
Absorption coefficient [mm^{-1}]	1.278
F[000]	1256
λ(Mo-K_α) [Å]	0.71073
Largest diff peak/hole [e Å^{-3}]	0.639/–0.514
No. independent reflections	5614
No. reflections [I > 2.0σ(*I*)]	4962
R_1	0.0294
wR_2	0.0768
Goodness-of-fit on F^2	1.037

Spectrofluorimetric Measurements: Fluorescence emission spectra were recorded at 25 °C with a Perkin–Elmer LS50B spectrofluorimeter equipped with a Hammamastu R928 photomultiplier. The lin-

earity of the fluorescence emission versus the concentration was checked in the concentration range 0 to 10^{-6} mol L^{-1}. Emission spectra were normalised by the manufacturer-supplied correction curves. Quantum yields were determined by comparison of the integrated corrected emission spectrum of standard quinine sulfate[51] [the quantum yield (Φ) is 0.55]. Spectrofluorimetric pH titrations of the ligand and the complex were performed as follows: the stock solutions of the ligand or the complex (ca. 3×10^{-5} mol L^{-1}) were prepared by dissolving an appropriate amount of the ligand in a 50-mL volumetric flask and by diluting with degassed water under an argon atmosphere. The titration solution {[LH] = 5×10^{-7} mol L^{-1}} was prepared by appropriate dilution of the stock solution. The response of LH to increased amounts of Zn^{2+} was checked as follows: successive volumes of $Zn(ClO_4)_2\cdot6H_2O$ (1.2×10^{-3} mol L^{-1}) were added to ligand solutions (3×10^{-5} mol L^{-1}) for a constant pH value [CAPS buffer solution (2×10^{-2} mol L^{-1})]. These solutions were further diluted in CAPS buffer in order to reach a LH concentration of 5×10^{-7} mol L^{-1}. The emission spectra of ligand and complex solutions were recorded after excitation at a wavelength of λ = 270 nm in the range 275–400 nm (slit width of 5 nm).

Supporting Information (see footnote on the first page of this article): The ^{1}H NMR spectra of LH as well as the ^{1}H NMR spectra of a mixture of LH and Zn^{2+} as a function of pH. A comparison of the affinities of LH and cyclen for Zn^{II} is also reported.

Acknowledgments

We thank H. Ballia and D. Harakat (Université de Reims Champagne Ardenne, France) for their help with the NMR 2D measurements and with ESI-MS measurements, respectively. T. Roisnel is gratefully acknowlegded for the crystal structure determination. Prof. S. Aoki (Tokyo University of Science), Dr. C. Picard (Université Paul Sabatier, Toulouse, France) and Prof. J. Rimbault (Université de Reims Champagne Ardenne, France) are gratefully acknowledged for helpful discussions.

[1] A. W. Czarnik, *Fluorescent Chemosensors for Ion and Molecule Detection*, American Chemical Society, Washington DC, **1993**.
[2] L. Fabbrizzi, A. Poggi, *Chem. Soc. Rev.* **1995**, *24*, 197–202.
[3] A. W. Czarnik, *Acc. Chem. Res.* **1994**, *27*, 302–308.
[4] A. P. De Silva, H. Q. N. Gunaratne, T. Gunnlaugsson, A. J. Huxley, C. P. Mc Coy, J. T. Rademacher, T. E. Rice, *Chem. Rev.* **1997**, *97*, 1515–1566.
[5] B. Valeur, I. Leray, *Coord. Chem. Rev.* **2000**, *205*, 3–40.
[6] E. Kimura, T. Koike, *Chem. Soc. Rev.* **1998**, *27*, 179–184.
[7] P. Jiang, Z. Guo, *Coord. Chem. Rev.* **2004**, *248*, 205–229.
[8] E. H. Cox, G. L. Mc Lendon, *Curr. Opin. Chem. Biol.* **2000**, *4*, 162–165.
[9] J. E. Coleman, *Curr. Opin. Chem. Biol.* **1998**, *2*, 222–234.
[10] S. J. Lippard, J. M. Berg, *Principles of Bioionorganic Chemistry*, De Boeck University, Brussels, **1997**.
[11] S. Burdette, S. J. Lippard, *Coord. Chem. Rev.* **2001**, *216–217*, 333–361.
[12] a) P. D. Zalewski, I. J. Forbes, W. H. Betts, *Biochem. J.* **1993**, *296*, 403–408; b) M. S. Nasir, C. J. Fahrni, D. A. Suhy, K. J. Kolodsick, C. P. Singer, T. V. O'Halloran, *J. Biol. Inorg. Chem.* **1999**, *4*, 775–783; c) C. J. Fahrni, T. V. O'Halloran, *J. Am. Chem. Soc.* **1999**, *121*, 11448–11458.
[13] a) P. Coyle, P. D. Zalewski, J. C. Phicox, I. J. Forbes, A. D. Ward, S. F. Lincoln, I. Mahadevan, A. M. Rofe, *Biochem. J.* **1994**, *303*, 781–786; b) T. Hirano, K. Kikuchi, Y. Urano, T. Higichi, T. Nagano, *Angew. Chem. Int. Ed.* **2000**, *39*, 1052–1055.
[14] E. U. Akkaya, M. E. Huston, A. W. Czarnik, *J. Am. Chem. Soc.* **1990**, *112*, 3590–3593.
[15] T. Koike, T. Watanabe, S. Aoki, E. Kimura, M. Shiro, *J. Am. Chem. Soc.* **1996**, *118*, 12696–12703.
[16] S. Aoki, S. Kaido, H. Fujioka, E. Kimura, *Inorg. Chem.* **2003**, *42*, 1023–1030.
[17] S. Aoki, K. Sakurama, N. Matsuo, Y. Yamada, R. Takasawa, S. Tanuma, M. Shiro, K. Takeda, E. Kimura, *Chem. Eur. J.* **2006**, *12*, 9066–9080.
[18] M. Le Baccon, F. Chuburu, L. Toupet, H. Handel, M. Soibinet, I. Déchamps-Olivier, J. P. Barbier, M. Aplincourt, *New J. Chem.* **2001**, *25*, 1168–1174.
[19] a) R. Fournaise, C. Petitfaux, *Talanta* **1987**, *34*, 385–395; b) R. Fournaise, C. Petitfaux, *Analusis* **1990**, *18*, 242–249.
[20] A. Bianchi, M. Micheloni, P. Paoletti, *Coord. Chem. Rev.* **1991**, *110*, 17–113.
[21] a) S. El Ghachtouli, C. Cadiou, I. Déchamps-Olivier, F. Chuburu, M. Aplincourt, T. Roisnel, *Eur. J. Inorg. Chem.* **2006**, 3472–3481; b) M. Shionoya, T. Ikeda, E. Kimura, M. Shiro, *J. Am. Chem. Soc.* **1994**, *116*, 3848–3859.
[22] J. Catalán, R. M. Claramunt, J. Elguero, J. Laynez, M. Menéndez, F. Anvia, J. H. Quian, M. Taagepera, R. W. Taft, *J. Am. Chem. Soc.* **1988**, *110*, 4105–4111.
[23] T. J. Lane, K. P. Quinlan, *J. Am. Chem. Soc.* **1960**, *82*, 2994–2997.
[24] M. Krishnamurthy, P. Phaniraj, S. K. Dogra, *J. Chem. Soc. Perkin Trans. 2* **1986**, 1917–1925.
[25] a) M. R. Figueroa, D. E. Gomez, C. P. Iglesias, A. De Blas, T. R. Blas, *Eur. J. Inorg. Chem.* **2007**, 2198–2207; b) G. Berden, W. L. Meerts, E. Jalviste, *J. Chem. Phys.* **1995**, *103*, 9596–9606; c) J. R. Platt, *J. Chem. Phys.* **1951**, *19*, 101–118.
[26] M. Alvaro, H. García, E. Palomares, R. Achour, A. Moussaif, R. Zniber, *Chem. Phys. Lett.* **2001**, *250*, 240–246.
[27] H. Walba, R. W. Isensee, *J. Org. Chem.* **1961**, *26*, 2789–2791.
[28] A. E. Goeta, J. A. K. Howard, D. Maffeo, H. Puschmann, J. A. G. Williams, D. S. Yufit, *J. Chem. Soc. Dalton Trans.* **2000**, 1873–1880.
[29] V. J. Thöm, C. C. Fox, J. C. A. Boeyens, R. D. Hancock, *J. Am. Chem. Soc.* **1984**, *106*, 3198–3207.
[30] G. Golub, H. Cohen, P. Paoletti, A. Bencini, L. Messori, I. Bertini, D. Meyerstein, *J. Am. Chem. Soc.* **1995**, *117*, 8353–8361.
[31] S. Aoki, K. Iwaida, N. Hanamoto, M. Shiro, E. Kimura, *J. Am. Chem. Soc.* **2002**, *124*, 5256–5257.
[32] X. P. Yang, B. S. Kang, W. K. Wong, C. Y. Su, H. Q. Liu, *Inorg. Chem.* **2003**, *42*, 169–179.
[33] T. Matsubara, K. Hirao, *J. Mol. Chem. Theochem.* **2002**, *581*, 203–213.
[34] Q. X. Li, Q.-H. Luo, Y. Z. Li, C. Y. Duan, Q. Y. Tu, *Inorg. Chim. Acta* **2005**, *358*, 504–512.
[35] T. Koike, S. Kajitani, I. Nakamura, E. Kimura, M. Shiro, *J. Am. Chem. Soc.* **1995**, *117*, 1210–1219.
[36] J. Moreau, E. Guillon, J. C. Pierrard, J. Rimbault, M. Port, M. Aplincourt, *Chem. Eur. J.* **2004**, *10*, 5218–5232.
[37] T. Koike, M. Takamura, E. Kimura, *J. Am. Chem. Soc.* **1994**, *116*, 8443–8449.
[38] E. K. Barefield, H. C. Freeman, D. G. V. Derveer, *Inorg. Chem.* **1986**, *25*, 552–558.
[39] D. Meyerstein, *Coord. Chem. Rev.* **1999**, *185–186*, 141–147.
[40] M. F. Hoq, R. E. Shepherd, *Inorg. Chem.* **1984**, *23*, 1851–1858.
[41] A. P. de Silva, H. Q. N. Gunaratne, T. Gunnlaugsson, A. J. M. Huxley, C. P. Mc. Coy, J. T. Rademacher, T. E. Rice, *Chem. Rev.* **1997**, *97*, 1515–1566.
[42] S. Aoki, D. Kagata, M. Shiro, K. Takeda, E. Kimura, *J. Am. Chem. Soc.* **2004**, *126*, 13377–13390.
[43] N. C. Lim, H. C. Freake, C. Bruckner, *Chem. Eur. J.* **2005**, *11*, 38–49.
[44] J. A. Kemio, T. M. Shepherd, *Chem. Phys. Lett.* **1977**, *47*, 158–162.

[45] *COLLECT*, KappaCCD software, Nonius BV, Delft, The Netherlands, **1998**.
[46] Z. Otwinowski, W. Minor in *Methods in Enzymology* (Ed.: C. W. Carter Jr, R. M. Sweet), Academic Press, New York, **1997**, vol. 276, pp. 307.
[47] A. Altomare, M. C. Burla, M. Camalli, G. Cascarano, C. Giacovazzo, A. Guagliardi, A. G. G. Moliterni, G. Polidori, R. Spagna, *J. Appl. Crystallogr.* **1999**, *32*, 115.
[48] G. M. Sheldrick, *SHELX97, Program for the Refinement of Crystal Structures*, University of Göttingen, Germany, **1997**.
[49] A. J. M. Duisenberg, *Reflections on Area detectors*, PhD Thesis, Utrecht, **1998**.
[50] G. M. Sheldrick, *SADABS version 2.03*, Bruker AXS Inc., Madison, Wisconsin, USA, **2002**.
[51] P. C. Tway, L. J. Cline Love, *J. Phys. Chem.* **1982**, *86*, 5223–5226.

Received: June 13, 2007
Published Online: September 21, 2007

